Evaluating Path Loss Models in Heterogeneous Environments: A Land Cover Segmentation Approach

Samuel S. Troina[1], Maiquel S. Canabarro[2], Felipe S. Marques[1]

[1]Technological Development Center – Federal University of Pelotas (UFPEL)
96010-610 – Pelotas – RS – Brazil

[2]Engineering Center
Federal University of Pelotas (UFPEL) – Pelotas, RS – Brazil

{samuel.troina,canabarrom}@gmail.com, felipem@inf.ufpel.edu.br

Abstract. *Path loss models are advantageous for analyzing complex environments and offer valuable network planning and optimization insights. Given the numerous challenges, predictive models incorporating environmental characteristics are essential for more accurate results. This study compares the accuracy of traditional predictive models, such as Free Space and Log-Distance, against the Log-Distance Multi-Exponent model using signals transmitted by LoRa technology. The ability of the latter model to classify the terrain coverage into distinct categories makes it particularly relevant in complex environments. Initially, the laboratory performed device calibration, followed by measurement campaigns in environments characterized by obstructed and unobstructed paths. The results indicate that segmenting the signal path based on terrain coverage is a practical approach that provides greater precision in estimating signal loss. Specifically, a path-segmented predictive model demonstrated a mean absolute error of 2 dB for environments with uniform land cover, outperforming the Free Space Model by 65%. Similarly, for mixed coverage, the Mean Absolute Error was 2.96 dB, representing a significant improvement, exceeding the Free Space Model by 75.6% and the Log-Distance model by 32.1%. These findings validate the effectiveness of the Log-Distance Multi-Exponent model, contributing to enhanced network planning efficiency.*

1. Introduction

Economy 4.0 encompasses various sectors, including smart cities, agribusiness, industries, healthcare, logistics, and more. A key pillar of this economy is connectivity, which enables the integration and exchange of information between various systems and devices [Aqeel-ur Rehman and Shaikh 2014].

Wireless networks, particularly Low Power Wide Area Networks (LPWANs), have garnered significant attention from the scientific community because of their capability for long-range communication with low power consumption. Among LPWAN technologies, LoRa has received considerable emphasis [Kais Mekki and Meyer 2019]. However, deploying networks effectively in environments with heterogeneous land cover presents challenges. Dense vegetation, topography, natural obstacles, and interference can significantly affect signal propagation, reducing signal strength and affecting network performance [Kurt and Tavli 2017].

Deploying a wireless network requires careful analysis of the dynamics of signal propagation, considering the specific characteristics of the environment. Understanding and evaluating the impact of diverse terrain conditions is critical in environments with heterogeneous land cover. This study investigates LoRa signal propagation, aiming to provide accurate modeling and characterization of the signal. Under these circumstances, it can offer valuable insights for network planning, sizing, and optimization, ensuring reliable and efficient communication in challenging environments [Mortazavi et al. 2015].

Traditionally, the implementation of a network begins with a site survey, which involves measuring signal strength and transmission quality at predetermined points. However, this process relies on human and financial resources to be carried out, in addition to the precise selection of the analyzed points of interest, which must be accessible and representative.

In this context, path loss models that characterize signal propagation behavior offer advantages in analyzing complex environments. Implementing a network can present challenges due to difficulties accessing the environment, high costs, and the time required for traditional measurement methods. In such cases, using reliable predictive models becomes indispensable [Konak 2009].

Given the highlighted challenges, it is evident that models considering the particularities of LPWAN technologies and environmental characteristics are necessary to obtain more accurate and reliable results. Such models contribute to more efficient network node positioning planning and ensure optimal connectivity.

This study evaluates the accuracy and reliability of predictive path loss models in heterogeneous land cover environments. Specifically, it compares the Free Space, Log-Distance, and Log-Distance Multi-Exponent models with empirical data collected from a region with mixed land cover. Additionally, the study includes comparisons with the Irregular Terrain Model (ITM) using CloudRF[1] software and results from the Radio Mobile[2] tool. An essential contribution of this work is its emphasis on device calibration — a crucial yet often overlooked step — to ensure data quality and enhance model reliability.

2. Related Work

Environmental characteristics and phenomena directly impact signal strength attenuation during propagation. In the Log-Distance Model, these influences are represented by a parameter known as the path loss exponent, which quantifies the signal decay rate. The path loss exponent typically ranges from 2 to 6, with lower values (around 2) corresponding to ideal conditions, such as line-of-sight (LOS) propagation, where obstacles and attenuation factors are minimal. Conversely, higher values are observed in environments with significant attenuation factors, such as dense vegetation, complex topography, or urban areas, where signal propagation is obstructed and scattered [Sirdeshpande and Udupi 2016].

Several studies aim to characterize LoRa signal propagation under various conditions and aspects. For instance, [El Chall et al. 2019] analyzed the impact of antenna height on signal attenuation and proposed modifying the Log-Normal model by introducing a variable that relates signal loss to antenna height. Their study focused on a single

[1] https://cloudrf.com
[2] https://www.ve2dbe.com

parameter of the LoRa transmitter, evaluating its behavior in different urban, rural, and indoor environments.

Studies have also compared model performance using empirical data against predictions. For example, [Batalha et al. 2022] evaluated the Free Space, Log-Distance, and Okumura-Hata models in an urban area, assessing their accuracy under real-world conditions. Similarly, [Kramm et al. 2023] analyzed the performance of the RadioPlanner software by comparing its predictions with empirical results obtained from field measurements conducted in an area with irregular terrain. Their findings indicate that while the software demonstrates good predictability for line-of-sight links, its performance significantly decreases in scenarios with obstructions, showing reduced accuracy.

[Elijah et al. 2021] analyzed the diurnal variation and the effects of weather conditions on a LoRa link configured in a LoRaWAN network. The study addressed the impact of factors such as device temperature, atmospheric temperature, relative humidity, solar radiation, and rain on the performance of the LoRa communication link by observing RSSI values.

[Ferreira et al. 2020] investigated LoRa signal propagation in forest, urban, and suburban vehicular environments. These environments were selected due to their diverse propagation conditions, and the study also included scenarios involving mobile nodes. To characterize the communication link, metrics such as the Received Signal Strength Indicator (RSSI), Signal-to-Noise Ratio (SNR), and Packet Delivery Ratio (PDR) were analyzed.

[Myagmardulam et al. 2021] presents a model in which the transmission distance is divided into two classes: line-of-sight and those with total or partial obstruction. The identification of the segments occurs through the analysis of data obtained with a Digital Surface Model (DSM). The path loss of the line-of-sight group is determined using the Free Space model, while segments with obstruction are determined and compared with the Weissberger, ITU-R, COST235, FITU-R, and lateral ITU-R models.

[Demetri et al. 2019, Lin et al. 2021, Liu et al. 2021] used AI to classify the land cover along a signal path, for example, in vegetation, open fields, roads, water, and buildings, and to segment it by land cover classification. In [Demetri et al. 2019], the land cover is classified into two groups: line-of-sight (LOS) and non-line-of-sight (NLOS). This segmentation determines which variation of the Okumura-Hata model to use.

[Lima et al. 2024] conducted a study to characterize uplink transmissions addressing IoT connectivity demands in the Amazon River region. Their results were compared with the Log-Distance, Floating Intercept, and Okumura-Hata models to evaluate performance. Additionally, the authors proposed a novel propagation model to predict signal losses caused by vegetation. This model builds upon the Free Space model, incorporating vegetation attenuation calculated using the recommendations outlined in ITU-R P.833.

3. Experimental Setup

To measure LoRa signal propagation, we developed a prototype communication device using a LoRa module commercialized by Reading. We chose this module because Brazilian regulatory agency laws certify it. The device incorporates an ESP8266-01 module, as shown in Figure 1(a), to control and interface with the LoRa module.

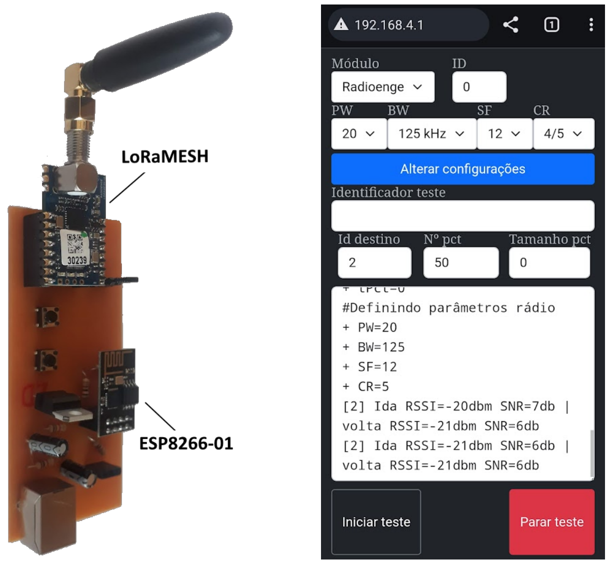

(a) Prototype device (b) Prototype Control System

Figure 1. Prototype device and interface of control system.

All tests were conducted according to Brazilian regulations and employing the LoRaWAN AU915-928 standard, with a particular emphasis on communication directed toward the gateway. During data collection, the devices were equipped with 3 dBi antennas and placed 1.5 meters above ground level. They remained stationary throughout the tests to ensure better stability in the results and mitigate potential Doppler effect impacts on transmissions, as highlighted in the research by [Petäjäjärvi et al. 2017].

We collected 20 received signal strength (RSSI) samples at different distances, with measurements taken at 5-second intervals. Additionally, we explored how transmission power influences received signal strength by adjusting transmitting power levels within the range of 11 dBm to 20 dBm in increments of 3 dBm. We chose this range to align with the principle that each 3 dBm reduction in transmission power halves the power in Watts, as the power law describes.

To evaluate the performance of the path loss models, we used the metrics Mean Absolute Error (MAE), Mean Absolute Percentage Error (MAPE), Mean-Square Error (MSE), and Root Mean-Square Error (RMSE). These metrics provided comprehensive insights into the model's accuracy and effectiveness in predicting signal propagation.

3.1. Device Calibration

We analyzed and measured the actual transmission power level of the LoRa module. As a spectrum analyzer with the required precision was unavailable, we performed tests using a pair of LoRa modules interconnected directly by a cable. These tests collected 200 samples of RSSI values using different transmission powers (11 dBm - 20 dBm), spreading factors (SF7 - SF10), CR 4/5, and BW 125. Figure 2 depicts the setup used, where the transceiver module is consistently connected to a 30 dB power attenuator, as the maximum power supported by the module is 10 dBm.

It is essential to highlight that the results obtained in the analysis reflect approxi-

Figure 2. A pair of LoRa modules is interconnected directly by a cable with a 30 dB attenuator.

mate values due to the precision limitations of the equipment used. However, these measurements provided a closer estimation of the actual transmission power than the nominal values specified in the datasheet.

The evaluation of the transmission power of the LoRa module revealed that it did not exceed 14 dBm, even though it was configured for transmission at 20 dBm, as specified in the module's datasheet. Additionally, we observed that the spreading factor influenced the transmission power, with the module's output varying according to the parameterized spreading factor. Table 1 presents the correlations identified, which we used as references for the employed transmission power.

Table 1. Correlation between the parameterized powers and those measured

PW	SF 10	SF 9	SF 8	SF 7
20 dBm	7.50 dBm	8.15 dBm	8.69 dBm	13.64 dBm
17 dBm	6.64 dBm	7.48 dBm	8.01 dBm	12.77 dBm
14 dBm	4.87 dBm	5.08 dBm	5.91 dBm	9.50 dBm
11 dBm	2.42 dBm	2.87 dBm	3.58 dBm	7.33 dBm

3.2. Reference Campaign

This campaign aimed to enhance the reliability of the collected data by analyzing signal behavior in line-of-sight (LOS) conditions, using the Free Space model as a benchmark. It was conducted at Cassino Beach in Rio Grande, Rio Grande do Sul, Brazil, chosen for its expansive, flat, and obstacle-free sandy terrain, ideal for LOS conditions (Figure 3). Conducting the tests in this environment facilitated a more precise evaluation of signal attenuation, free from interference caused by obstacles. As a result, it closely reflected signal attenuation in an obstruction-free environment.

The measurements in this campaign followed a predefined methodology, with distances ranging from 1 to 5 meters between the devices. Table 2 presents the average of one hundred RSSI samples at a distance of 1 meter across various transmission power and spreading factor configurations. The path loss (PL) is calculated using equation 1, where the average RSSI value is applied in the term corresponding to the received power. This equation $P_{t(dBm)}$ represents the transmission power, $G_{t(dBi)}$ and $G_{r(dBi)}$ denote transmitter and receiver antenna gains, and P_r is the received signal strength at the receiver.

$$PL(dB) = P_{t(dBm)} + G_{t(dBi)} + G_{r(dBi)} - P_{r(dBm)} \tag{1}$$

To determine the Effective Isotropic Radiated Power (EIRP), we used the Equation

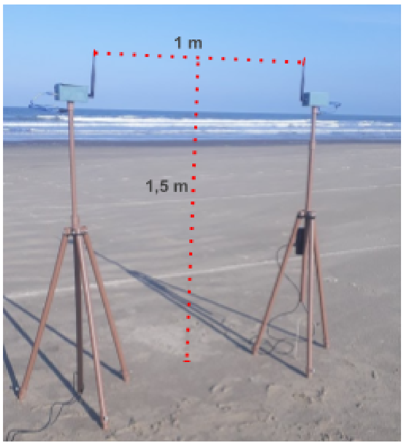

Figure 3. Devices test position in LOS conditions.

2.

$$ERIP = P_{t(dBm)} + G_{t(dBi)} \tag{2}$$

Table 2. The measurements of collecting the referential PL values at 1 meter

BW 125 khz												
Pt	RSSI (dBm)				IRL(dBm) = RSSI - 3dBi				PL(dB) = EIRP - IRL			
	SF 10	SF 9	SF 8	SF 7	SF 10	SF 9	SF 8	SF 7	SF 10	SF 9	SF 8	SF 7
20	-21.4	-20.7	-20.3	-15.4	-24.4	-23.7	-23.3	-18.4	34.9	34.9	35.0	35.1
17	-22.8	-22.1	-21.6	-16.6	-25.8	-25.1	-24.6	-19.6	35.4	35.6	35.6	35.4
14	-26.9	-26.9	-26.3	-20.6	-29.9	-29.9	-29.3	-23.6	37.8	38.0	38.2	36.1
11	-26.8	-26.4	-25.6	-21.8	-29.8	-29.4	-28.6	-24.8	35.2	35.3	35.2	35.1

Analyzing the results obtained at a distance of 1 meter, it is evident that the signal intensity losses exceed the predicted value of 31.56 dB by the Free Space model. The closest value obtained was 34.91 dB when using a transmission power of 20 dBm combined with a spreading factor of 10. However, even though the value is close, there is a significant difference compared to the theoretical model, being approximately 10.6% larger.

Therefore, to compensate for the difference identified between the measured values and those expected for a LOS environment, a correction factor (CF) was determined, which corresponds to the difference between the path loss obtained in the collection at 1 meter and the path loss calculated by the Free Space model, using equation 3.

$$CF = PL(Measured) - PL(Free\ Space) \tag{3}$$

Table 3 shows the correction factors that must be added to the measured RSSI values to reduce the difference, according to the parameterized power and spreading factor.

3.3. Evaluation Campaign

In this campaign, the objective was to analyze the influence of different land covers on signal propagation, with a specific focus on the impact of vegetation. The study area

Table 3. Calculated correction factors with BW 125 KHz

FSPL(dB)	Pt (dBm)	PL(dB)				CF(dB) = PL - FSPL			
		SF 10	SF 9	SF 8	SF 7	SF 10	SF 9	SF 8	SF 7
31.56	20	34.91	34.89	34.98	35.06	3.35	3.34	3.42	3.50
	17	35.42	35.62	35.60	35.41	3.86	4.07	4.05	3.85
	14	37.79	37.96	38.24	36.06	6.23	6.40	6.68	4.50
	11	35.17	35.30	35.15	35.15	3.61	3.74	3.60	3.59

chosen for this analysis was the "Vila Assumpção" neighborhood in Pelotas, Rio Grande do Sul, Brazil. The campaign investigated three distinct scenarios based on the land cover in each area: open field, characterized by low and sparse vegetation; forest, with dense tree cover; and mixed, featuring a combination of low and sparse vegetation along with dense tree cover. Figure 4 displays the two types of land cover found in the area. Figure 4(a) illustrates the open field land cover, while Figure 4(b) represents the forest cover.

(a) Open field

(b) Forest

Figure 4. Types of land cover present in the environment.

The satellite view of the environment, illustrated in Figure 5, highlights the test locations and the placement of the gateway and the end devices. Table 4 provides a detailed overview of the analyzed point combinations and their distances. Currently, our automated method for path segmentation is under development. This way, we manually segmented the land cover distances. It indicates the associated distances for each land coverage type and each test's measured RSSI and Path Loss (PL).

The performance evaluation of the models enabled the identification of their accuracy and determination of the model that yields better results when applied to long-distance links with variations in land coverage. One notable feature of the evaluated models, excluding the Free Space model, is the presence of a power decay exponent (n). This exponent plays a crucial role in determining the rate at which signal strength decreases with distance. Accurate determination of the n value is essential for improving the precision of the models.

To determine the optimal value n, we employed the curve fitting technique using the least squares method provided by the SciPy library (https://scipy.org/). Table 5 displays the Path Loss (dB) at the referential distance (1m), denoted by $PL(d_0)$, and

Table 4. Links evaluated in the data collection campaign as illustrated in Figure 5

	Devices		Land cover Distance			Mesuread RSSI (dBm)		
Id	Gateway	End Device	Open field	Forest	Total	Min	Mean	Max
1	GW1	P1	65 m	-	65 m	-63	-57	-50
2	GW1	P2	184 m	-	184 m	-75	-68	-62
3	GW1	P3	252 m	-	252 m	-82	-77	-72
4	GW1	P4	389 m	-	389 m	-82	-76	-71
5	GW2	P5	-	50 m	50 m	-60	-54	-47
6	GW2	P6	-	170 m	170 m	-80	-75	-68
7	GW2	P7	-	288 m	288 m	-95	-89	-83
8	GW3	P8	110 m	75 m	185 m	-85	-77	-71
9	GW3	P9	239 m	75 m	314 m	-82	-76	-69

the calculated values of n. These values are derived from measurements obtained in the campaigns, segmented by type of coverage. The dataset and the notebook are in the repository[3], which contains all the analyses performed.

Table 5. Samples of $PL(d_0)$, d_0 and n by land cover and power for the SF 10 and 7

	Open field		Forest	
PW	SF 10	SF 7	SF 10	SF 7
20	20.52, 2.07, 2.67	15.22, 1.99, 3.01	10.20, 4.19, 4.31	9.02, 4.62, 4.67
17	20.92, 2.07, 2.62	16.86, 2.42, 3.08	13.37, 4.76, 4.26	3.18, 3.59, 4.78
14	19.39, 1.99, 2.60	16.45, 2.18, 2.95	9.27, 4.38, 4.31	0.79, 3.92, 4.93
11	18.95, 1.83, 2.71	20.48, 2.84, 2.99	13.37, 4.73, 4.32	7.81, 4.34, 4.74

The graphs in Figure 6 illustrate that higher spreading factors result in a slower signal decay rate than lower spreading factors. This finding emphasizes the importance of carefully selecting the parameter n to align with the specific LoRa configuration, ensuring optimal performance under varying conditions.

We evaluated the models using specific reference values for each land coverage type and parameterized the LoRa transceiver. These evaluations were conducted separately, initially focusing on links with homogeneous coverage and then considering links with mixed land coverage.

The Free Space model assumes ideal conditions with line-of-sight propagation, where the distance between the transmitter and receiver [Friis 1946]. In contrast, the Log-Distance model accounts for more complex environments by introducing a path loss exponent that reflects the impact of obstacles, terrain, and other environmental factors on signal propagation [Rappaport 2002]. Building on this, the Log-Distance Multi-Exponent model extends the standard Log-Distance model, incorporating multiple path loss exponents, each corresponding to different land-cover types encountered along the propagation path. This iterative approach provides a more accurate representation of heterogeneous environments by segmenting the link into sections, each with its specific propagation characteristics, and summing the cumulative losses [Lin et al. 2021], as expressed in 4.

[3]https://anonymous.4open.science/r/paper_pl_evaluation-CC17

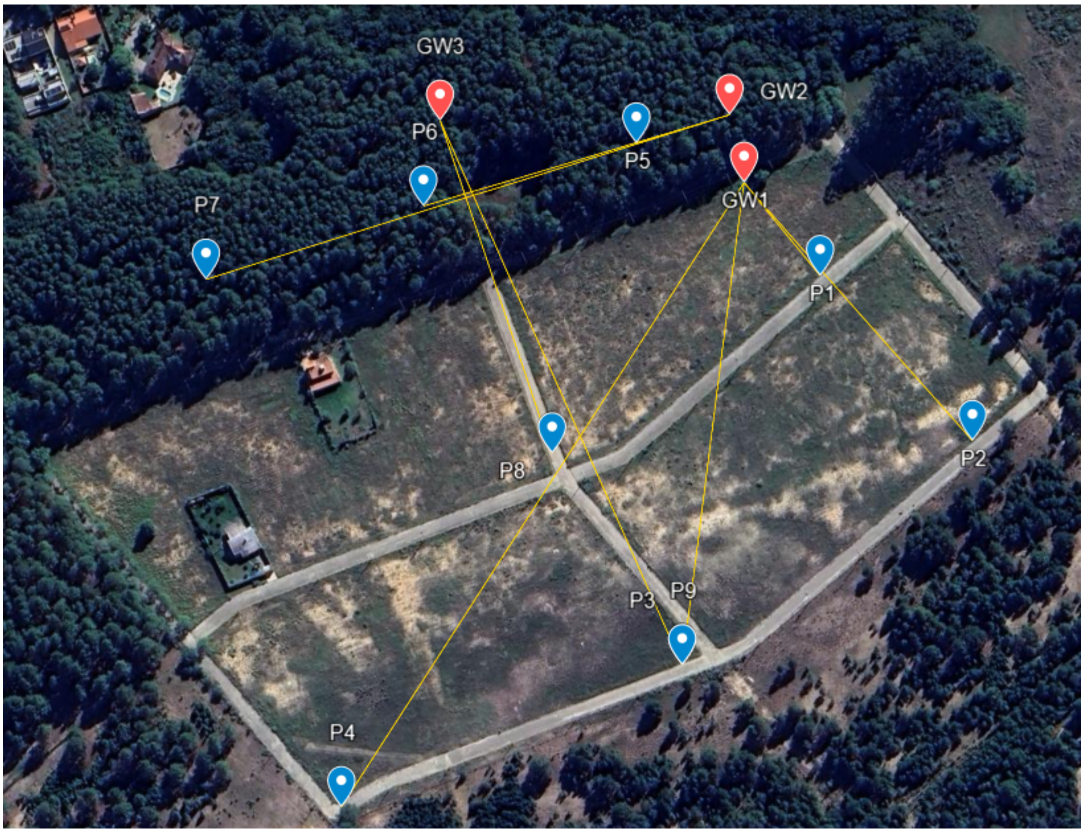

Figure 5. Position of the gateway (red mark) and the end devices (blue mark).

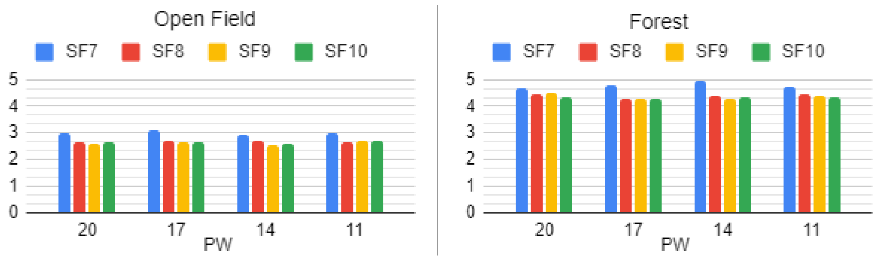

Figure 6. Graph of path loss exponents by coverage

$$PL(d_K) = PL(d_0) + \sum_{k=i}^{K} \left(10n_{(d_{k-1},d_k)} \log_{10} \frac{d_k}{d_{k-1}} + N_{\sigma_{(d_{k-1},d_k)}} \right) \quad (4)$$

Where:

- d_1,d_2...d_k are the distances between a gateway and K consecutive positions along a link;
- $n_{(d_{k-1},d_k)}$ is the exponent of signal intensity loss relative to the class assigned to the link segment.

Table 6 shows the obtained Path Loss (PL) values. In this evaluation, we use link 9 as an example. The calculated PL value and their respective correction factors used the real transmission power presented in Table 1.

Table 6. PL evaluation of link 9 applying 20, 17, 14, and 11 dBm of power in the transmitter

Power	SF 10	SF 9	SF 8	SF 7	Mean
20 dBm	80.55 dB	78.51 dB	78.47 dB	81.94 dB	79.86 dB
17 dBm	78.28 dB	78.21 dB	79.06 dB	81.12 dB	79.16 dB
14 dBm	76.54 dB	76.78 dB	77.03 dB	80.50 dB	77.71 dB
11 dBm	78.51 dB	78.93 dB	80.38 dB	83.54 dB	80.34 dB

To demonstrate the applicability of the Log-Distance ME Model, equation 5 simulates the calculation of signal intensity loss. In this example, we considered data from link 9 when the transmission power of 20 dBm with a spreading factor of 10 was applied.

$$PL = 10.2 + 43.1 \log_{10} \frac{75}{4.19} + 26.7 \log_{10} \frac{314}{75} = 80.80\ dB \tag{5}$$

In the evaluation of link 9, the average RSSI observed was -76.40 dBm, corresponding to an average corrected path loss of 80.55 dB. Using the Log-Distance Multi-Exponent model for prediction, a path loss of 80.80 dB was estimated, showing a difference of only -0.25 dB from the measured value. For comparison purposes, when applying the Free Space and Log-Distance models in the same analysis, the estimated path losses were 81.50 dB and 82.84 dB, respectively.

In a practical application, this example illustrates that device calibration, combined with terrain segmentation and adopting a model that considers the environment's heterogeneity, provides predictions with greater accuracy and reliability.

Table 7 summarizes the results of the Free Space, Log-Distance, and Log-Distance Multi-Exponent models for links with single-type coverage. As anticipated, the analysis revealed that models derived from the Log-Distance approach demonstrated significantly better performance. Specifically, they achieved a Mean Absolute Error (MAE) 186% lower than the Free Space model. It shows the average magnitude of errors between predicted and observed values, expressed in the same unit as the measured variable. A lower MAE indicates smaller prediction errors and better model accuracy. This result underscores the reliability and precision of the Log-Distance-based models in predicting signal propagation.

Table 7. Performance evaluation of models in links with single-type coverage

PL Model	MAE (dB)	MAPE (%)	MSE (dB)	RMSE (dB)
FSPL	5.72	11	42.13	6.49
Log-Distance	2.00	3	6.67	2.58
Log-Distance ME	2.00	3	6.67	2.58

Based on the links in Table 4, which traverse mixed land coverages, Table 8 illustrates the model performances. These findings distinctly favor the Log-Distance Multi-Exponent model, showcasing superior accuracy. The MAE indicates an average deviation of 2.96 dB for mixed coverage, marking a notable enhancement, surpassing the Free Space Model by 75.67% and the Log-Distance by 32.1%.

Table 8. Performance evaluation of models in links with different land covers

Model	MAE (dB)	MAPE (%)	MSE (dB)	RMSE (dB)
FSPL	5.20	7	39.40	6.28
Log-Distance	3.91	5	15.66	3.96
Log-Distance ME	2.96	4	10.74	3.28

The accuracy of the Irregular Terrain Model (ITM), present in [Hufford 1999], was evaluated using the CloudRF and Radio Mobile software for links with heterogeneous terrain coverage. In the simulations, the CloudRF software predicted signal intensities for links 8 and 9 as -95 dBm and -101 dBm, respectively, as illustrated in Figure 7. The model exhibited errors of approximately 18 dB and 25 dB compared to the average measured values. These findings highlight that a link segmentation procedure yields more accurate results in such environments.

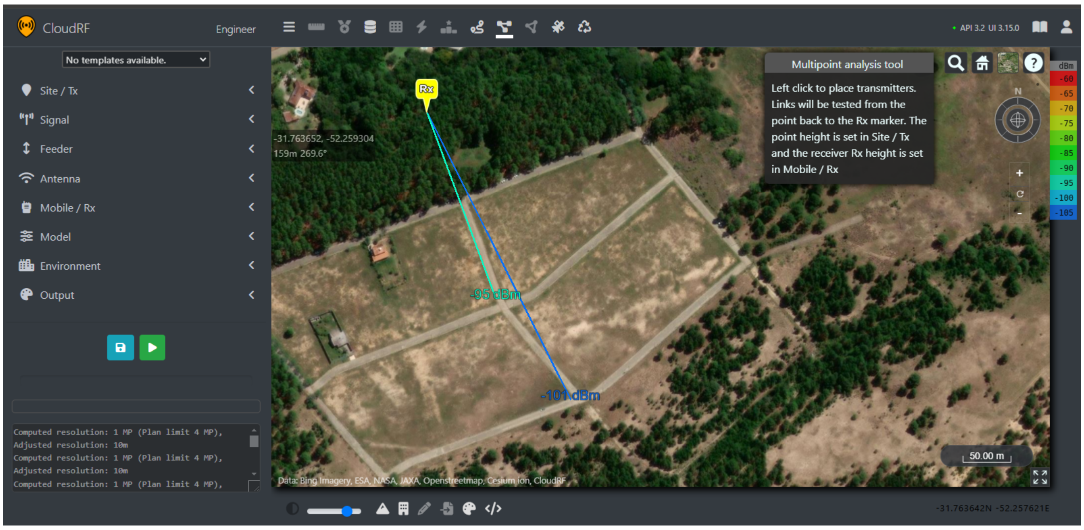

Figure 7. Validation of Irregular Terrain Model (ITM) on CloudRF.

The performance of the Radio Mobile tool was evaluated in links with heterogeneous coverage. Its results were less accurate than those of the CloudRF tool. As illustrated in Figures 8 and 9, the values obtained for links 8 and 9 were -106.78 dBm and -88.53 dBm, respectively.

4. Conclusions and Future Work

The results obtained from our evaluation offer valuable insights into model performance. They showcase the superiority of the Log-Distance Multi-Exponent model over the other evaluated models. This superiority underscores the efficacy of segmenting the signal path based on terrain coverage, a strategy that significantly enhances the accuracy of signal loss estimation when employing predictive models.

Other factors contributed to the enhanced precision observed in our results, including device calibration, the incorporation of correction factors, and the application of path loss exponents tailored to specific transmission parameter groups. These findings underscore the importance of considering land coverage characteristics and employing

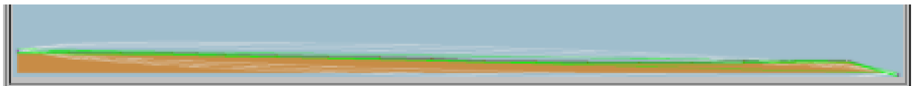

Link 8			
GW - Vila Assumpção (1)		(2) P8 - Vila Assumpção	
Latitude	-31.764005 °	Latitude	-31.765357 °
Longitude	-52.257521 °	Longitude	-52.256868 °
Ground elevation	13.5 m	Ground elevation	3.5 m
Antenna height	1.5 m	Antenna height	1.5 m
Azimuth	157.67 TN | 173.95 MG °	Azimuth	337.67 TN | 353.94 MG °
Tilt	-3.52 °	Tilt	3.52 °
Radio system			**Propagation**
TX power	20.00 dBm	Free space loss	75.86 dB
TX line loss	0.00 dB	Obstruction loss	42.91 dB
TX antenna gain	3.00 dBi	Forest loss	0.00 dB
RX antenna gain	3.00 dBi	Urban loss	0.00 dB
RX line loss	0.00 dB	Statistical loss	14.01 dB
RX sensitivity	-134.96 dBm	Total path loss	132.78 dB

Performance	
Distance	**0.162 km**
Precision	9.6 m
Frequency	915.200 MHz
Equivalent Isotropically Radiated Power	0.200 W
System gain	159.02 dB
Required reliability	90.000 %
Received Signal	-106.78 dBm
Received Signal	1.03 µV
Fade Margin	**26.24 dB**

Figure 8. Radio Mobile validation link 8.

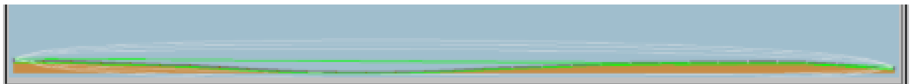

Link 9			
GW - Vila Assumpção (1)		(2) P9 - Vila Assumpção	
Latitude	-31.764005 °	Latitude	-31.766350 °
Longitude	-52.257521 °	Longitude	-52.256131 °
Ground elevation	13.5 m	Ground elevation	10.5 m
Antenna height	1.5 m	Antenna height	1.5 m
Azimuth	153.25 TN | 169.53 MG °	Azimuth	333.25 TN | 349.53 MG °
Tilt	-0.59 °	Tilt	0.59 °
Radio system			**Propagation**
TX power	20.00 dBm	Free space loss	80.94 dB
TX line loss	0.00 dB	Obstruction loss	18.60 dB
TX antenna gain	3.00 dBi	Forest loss	0.00 dB
RX antenna gain	3.00 dBi	Urban loss	0.00 dB
RX line loss	0.00 dB	Statistical loss	15.00 dB
RX sensitivity	-134.96 dBm	Total path loss	114.53 dB

Performance	
Distance	**0.292 km**
Precision	9.7 m
Frequency	915.200 MHz
Equivalent Isotropically Radiated Power	0.200 W
System gain	159.02 dB
Required reliability	90.000 %
Received Signal	-88.53 dBm
Received Signal	8.38 µV
Fade Margin	**44.49 dB**

Figure 9. Radio Mobile validation link 9.

appropriate models for path loss estimation, facilitating effective network planning and optimization across diverse environments.

Our future research will explore other environments and conditions to validate the quality and accuracy of the models under different aspects. Specifically, we plan to assess scenarios with rugged terrain to further analyze the impact of complex topographies on LoRa signal propagation. The correction results obtained so far have been satisfactory, reinforcing the applicability of the proposed approach. However, we emphasize the importance of characterizing radio performance in calibrated equipment for future studies, ensuring more precise and reliable model evaluations.

Acknowledgments

This work has been supported by the following Brazilian research agencies: FAPERGS, CAPES, and CNPq.

References

Aqeel-ur Rehman, Abu Zafar Abbasi, N. I. and Shaikh, Z. A. (2014). A review of wireless sensors and networks' applications in agriculture. *Computer Standards & Interfaces*, 36(2):236–270.

Batalha, I. d. S., Lopes, A. V. R., Lima, W. G., Barbosa, Y. H. S., De Alcântara Neto, M. C., Barros, F. J. B., and Cavalcante, G. P. S. (2022). Large-scale modeling and analysis of uplink and downlink channels for lora technology in suburban environments. *IEEE Internet of Things Journal*, 9(23):24477–24491.

Demetri, S., Picco, G. P., and Bruzzone, L. (2019). Laps: Lidar-assisted placement of wireless sensor networks in forests. *ACM Transactions on Sensor Networks*, 15(2):1–40.

El Chall, R., Lahoud, S., and El Helou, M. (2019). Lorawan network: Radio propagation models and performance evaluation in various environments in lebanon. *IEEE Internet of Things Journal*, 6(2):2366–2378.

Elijah, O., Rahim, S. K. A., Sittakul, V., Al-Samman, A. M., Cheffena, M., Din, J. B., and Tharek, A. R. (2021). Effect of weather condition on lora iot communication technology in a tropical region: Malaysia. *IEEE Access*, 9:72835–72843.

Ferreira, A. E., Ortiz, F. M., Costa, L. H. M. K., Foubert, B., Amadou, I., and Mitton, N. (2020). A study of the lora signal propagation in forest, urban, and suburban environments. *Annales des Telecommunications/Annals of Telecommunications*, 75(7-8):333 – 351. Cited by: 21; All Open Access, Green Open Access.

Friis, H. (1946). A note on a simple transmission formula. *Proceedings of the IRE*, 34(5):254–256.

Hufford, G. A. (1999). The its irregular terrain model, version 1.2.2: The algorithm. Technical report, Institute for Telecommunication Sciences.

Kais Mekki, Eddy Bajic, F. C. and Meyer, F. (2019). A comparative study of lpwan technologies for large-scale iot deployment. *ICT Express*, 5(1):1–7.

Konak, A. (2009). A kriging approach to predicting coverage in wireless networks. *International Journal of Mobile Network Design and Innovation*, 3(2):65–71.

Kramm, H., Feldman, M., Lima, R., Viana, L., Müller, I., and Ferreira, S. B. (2023). Evaluation of lora deployment through site survey on irregular terrain model. In *2023 XIII Brazilian Symposium on Computing Systems Engineering (SBESC)*, pages 1–6.

Kurt, S. and Tavli, B. (2017). Path-loss modeling for wireless sensor networks: A review of models and comparative evaluations. *IEEE Antennas and Propagation Magazine*, 59(1):18–37.

Lima, W. G., Lopes, A. V. R., Cardoso, C. M. M., Araújo, J. P. L., Neto, M. C. A., Tostes, M. E. L., Nascimento, A. A., Rodriguez, M., and Barros, F. J. B. (2024). Lora technology propagation models for iot network planningin the amazon regions. *Sensors*, 24(5).

Lin, Y., Dong, W., Gao, Y., and Gu, T. (2021). Sateloc: A virtual fingerprinting approach to outdoor lora localization using satellite images. *ACM Transactions on Sensor Networks*, 17(4).

Liu, L., Yao, Y., Cao, Z., and Zhang, M. (2021). Deeplora: Learning accurate path loss model for long distance links in lpwan. In *IEEE INFOCOM 2021 - IEEE Conference on Computer Communications*, pages 1–10.

Mortazavi, S. H., Salehe, M., and MacGregor, M. (2015). Maximum wsn coverage in environments of heterogeneous path loss. *International Journal of Sensor Networks*, 16(3):185–198.

Myagmardulam, B., Tadachika, N., Takahashi, K., Miura, R., Ono, F., Kagawa, T., Shan, L., and Kojima, F. (2021). Path loss prediction model development in a mountainous forest environment. *IEEE Open Journal of the Communications Society*, 2:2494–2501.

Petäjäjärvi, J., Mikhaylov, K., Pettissalo, M., Janhunen, J., and Iinatti, J. (2017). Performance of a low-power wide-area network based on lora technology: Doppler robustness, scalability, and coverage. *International Journal of Distributed Sensor Networks*, 13(3):1550147717699412.

Rappaport, T. S. (2002). *Wireless Communications: Principles and Practice*. Prentice Hall.

Sirdeshpande, N. and Udupi, V. (2016). Radio range mapping in wireless sensor networks. In *International Conference on Advances in Human Machine Interaction (HMI)*, pages 1–5. IEEE.